UNCLASSIFIED

AD 265 076

Reproduced
by the

ARMED SERVICES TECHNICAL INFORMATION AGENCY
ARLINGTON HALL STATION
ARLINGTON 12, VIRGINIA
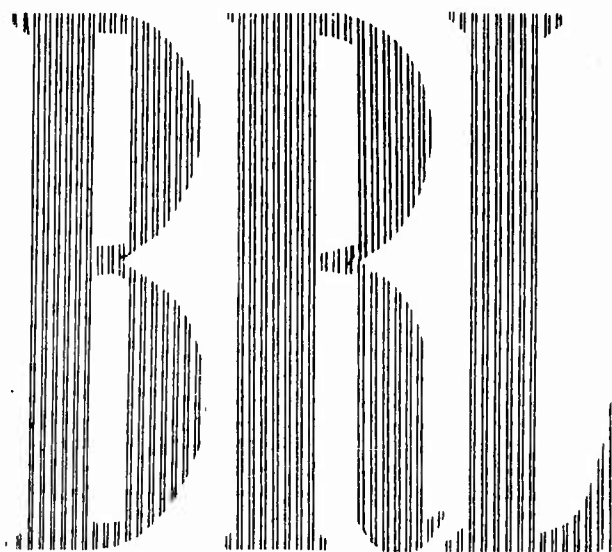
UNCLASSIFIED

BRL

REPORT NO. 1137
AUGUST 1961

TRANSIENT SKIN EFFECTS IN
EXPLODING WIRE CIRCUITS

F. D. Bennett

BALLISTIC RESEARCH LABORATORIES

ABERDEEN PROVING GROUND, MARYLAND

ASTIA AVAILABILITY NOTICE

Qualified requestors may obtain copies of this report from ASTIA.

BALLISTIC RESEARCH LABORATORIES

REPORT NO. 1137

AUGUST 1961

TRANSIENT SKIN EFFECTS IN EXPLODING WIRE CIRCUITS

F. D. Bennett

Exterior Ballistics Laboratory

ABERDEEN   PROVING   GROUND,   MARYLAND

BALLISTIC   RESEARCH   LABORATORIES

REPORT NO. 1137

FDBennett/bj
Aberdeen Proving Ground, Md
August 1961

TRANSIENT SKIN EFFECTS IN EXPLODING WIRE CIRCUITS

ABSTRACT

The transient response of the coaxial, current-measuring shunt commonly used in high-current, high frequency applications (up to 1 mc) is analyzed by Laplace transform methods. An approximate solution is obtained which allows estimates to be made of the errors expected. The current shunt measuring a damped oscillation will always report an initial current slope of zero, and the maximum rate of current rise is sensed shortly after switch-on. It is several percent low in typical cases. At the first current maximum, the shunt reading is a few tenths percent high and lags the impressed current by a small fraction of a cycle. The transient resistance of an idealized plate condenser is analyzed using the asymptotic solution for current. A numerical calculation indicates no alteration of initial conditions on the damped oscillation to arise from this source, so long as the characteristic damping time of the transient skin effect is small compared with the ringing time.

1. RESPONSE OF A COAXIAL CURRENT MEASURING RESISTANCE

The current pulse encountered in typical exploding wire experiments has a transient, irregular wave form with its basic frequency in or near the megacycle range and peak amplitude frequently greater than 10^4 amps. One desires to measure both current magnitude and pulse shape with high accuracy (within 2% of peak values) by means of a device which itself should add negligible impedance to the circuit and negligible perturbation to the current pulse.

Such a device would seem to be found in the coaxial shunt design given by Park,[1] which has found use in measurement of large currents at power frequencies and more recently in high current generators at about 60 kc[2] and in exploding wire experiments up to 20 kc basic frequency.[3,4,5]

Current shunts of this design are presently in use for the measurement of current pulses thru exploding wires in a circuit with ringing frequency of 446 kc.[6] While it might appear that the shunt technique is sufficiently well understood that no difficulties would occur in extending the method to 1/2 mc, certain discrepancies have been observed in the measurement of damped oscillations in the exploding wire circuit. These deviations from expected values have pointed to the necessity for better understanding of shunt characteristics under transient conditions, and have thus led directly to the present theoretical study.

In the modified design considered here (see Figure 1), the current measuring resistor consists of a short, hollow cylinder of nichrome V made the inner conductor at the shorted end of a coaxial stub which itself is connected into the circuit in series. Voltage sensing is accomplished by a small co-ax line entering through the shorted end, inside and coaxial with the nichrome element. In a particular example employed, the resistance of the nichrome element is about 10^{-3} ohm and its calculated inductive reactance less than 5% of the resistance at

5

1/2 mc. The nichrome tube is thin enough to indicate nearly constant resistance independent of skin effect at frequencies up to 1.5 mc yet strong enough to resist magnetic pinch forces from currents up to 10^5 amps.

When a study is made of the damped oscillations which can occur with the exploding wire replaced by a shorting bar, certain characteristic discrepancies are noted. The damping constant $\alpha = R/2L$ can be determined from comparison of successive current peaks and the angular frequency $\omega^2 = \omega_o^2 - \alpha^2$ where $\omega_o^2 = 1/LC$, from the time intervals between successive zeroes of the current curve. If capacity C is determined by an independent bridge measurement, the RLC constants of the circuits can be obtained without any recourse to actual current magnitudes. Yet when the values so obtained are used to predict the damped oscillation, one finds that the observed values of initial current slope are invariably smaller than the values predicted from circuit theory by amounts several times larger than the expected experimental error.

The theoretical treatment of the shunt, skin-effect problem, by Silsbee and Park[1] is based on the assumption of steady-state, continuous wave operation. Because of this limitation no conclusion can be drawn from their calculations as to the accuracy of a coaxial resistor for measuring switch-on transient pulses like those encountered in the exploding wire phenomenon. On the contrary, the study by Haines[7] of inverse skin effect for a solid cylindrical conductor carrying a steady oscillation, shows important differences between the initial current distribution and that which exists after transients have damped out. Thus the possibility exists that the response of a coaxial current-measuring shunt may be seriously in error at switch-on because of transient skin effect. This point of view is given some additional support by the work of Maninger[8] who studies the current distribution occurring in fine wires when applied current is a step function rising from - A to A at a given time.

5

1/2 mc. The nichrome tube is thin enough to indicate nearly constant resistance independent of skin effect at frequencies up to 1.5 mc yet strong enough to resist magnetic pinch forces from currents up to 10^5 amps.

When a study is made of the damped oscillations which can occur with the exploding wire replaced by a shorting bar, certain characteristic discrepancies are noted. The damping constant $\alpha = R/2L$ can be determined from comparison of successive current peaks and the angular frequency $\omega^2 = \omega_o^2 - \alpha^2$ where $\omega_o^2 = 1/LC$, from the time intervals between successive zeroes of the current curve. If capacity C is determined by an independent bridge measurement, the RLC constants of the circuits can be obtained without any recourse to actual current magnitudes. Yet when the values so obtained are used to predict the damped oscillation, one finds that the observed values of initial current slope are invariably smaller than the values predicted from circuit theory by amounts several times larger than the expected experimental error.

The theoretical treatment of the shunt, skin-effect problem, by Silsbee and Park[1] is based on the assumption of steady-state, continuous wave operation. Because of this limitation no conclusion can be drawn from their calculations as to the accuracy of a coaxial resistor for measuring switch-on transient pulses like those encountered in the exploding wire phenomenon. On the contrary, the study by Haines[7] of inverse skin effect for a solid cylindrical conductor carrying a steady oscillation, shows important differences between the initial current distribution and that which exists after transients have damped out. Thus the possibility exists that the response of a coaxial current-measuring shunt may be seriously in error at switch-on because of transient skin effect. This point of view is given some additional support by the work of Maninger[6] who studies the current distribution occurring in fine wires when applied current is a step function rising from - A to A at a given time.

In the present paper we consider the transient response of a coaxial resistive element to a current suddenly applied. Our treatment is closely modeled after that of Haines who employs the Laplace transform to obtain a general solution for the case of a solid cylindrical wire under arbitrary current excitation. While it appears that the tubular shunt problem can be exactly solved in principle, certain difficulties arise in the analysis which make it expedient to employ an approximate solution to obtain usable results in the practical cases considered. When this is done estimates can then be given of the accuracy to be expected from the coaxial, current measuring resistance during the early portion of a transient current pulse.

7

2. ANALYSIS

2.1 Formulation of the Problem

Consider the diffusion of magnetic field into a long cylindrical tube of metal of inner radius r and outer radius a. We employ cylindrical polar coordinates with z taken along, and r perpendicular to the axis of the tube. Then following Haines' treatment we assume Maxwell's equations (mks units), neglect displacement currents, set $\underline{B} = \mu\underline{H}$ and use Ohm's law, $i_z = \sigma E_z$, in a form which ignores both inertial effects of the current carriers and thermal diffusion. The relevant current equation for the i_z is then

$$\frac{1}{r}\frac{\partial}{\partial r}\left(r\frac{\partial i_z}{\partial r}\right) - \mu\sigma\frac{\partial i_z}{\partial t} = 0 \quad , \tag{1}$$

where t is time, $\mu = k_m\mu_o$ is the permeability and σ the conductivity of the medium. If we assume i_z to be independent of θ and z, which is reasonable on account of symmetry and because we wish currents anywhere along the tube to be the same, then conservation of charge plus the boundary conditions imply radial current everywhere zero.

For convenience introduce the change of variables $x = r/a$ and $y = t/\mu\sigma a^2$. Then Eq. (1) becomes

$$\frac{1}{x}\frac{\partial}{\partial x}\left(x\frac{\partial i_z}{\partial x}\right) - \frac{\partial i_z}{\partial y} = 0 \quad , \tag{2}$$

which is a form of the diffusion equation. The transformation on r is linear; whereas the time axis is compressed or expanded non-linearly depending on the values of μ, σ and a. Since the fundamental solutions will be expressed in terms of x and y, it is clear that to reach a given condition of current penetration will take much longer in media of large conductivity and dimension than when these values are small. Put another way, the solutions we shall obtain are self-similar in terms of the scaling parameter $\mu\sigma a^2$. We require solutions to Eq. (2) under the following boundary and initial conditions.

8

The total current $\mathcal{U}$, which may be arbitrarily specified, is found by integrating the current density over any cross-section of the tube and is

$$\mathcal{U}(y) = 2\pi a^2 \int_\epsilon^1 i_z(x,y) \, x dx \quad , \tag{3}$$

where $\epsilon = r_1/a$ denotes the inner boundary. Prior to switch-on both $\mathcal{U}$ and i_z must be identically zero. Thus

$$\left.\begin{array}{l} \mathcal{U}(y) = 0 \\[2mm] i_z(x,y) = 0 \end{array}\right\} \; y \leq 0 \quad . \tag{4}$$

Furthermore the radial derivative of current i_z must vanish at the inner boundary, and we write

$$\left(\frac{\partial i_z(x,y)}{\partial x}\right)_{x=\epsilon} = 0 \quad . \tag{5}$$

This last relation follows from Faraday's law $(\partial E_z/\partial r = \partial B_\phi/\partial t)$, Ohm's law $(i_z = \sigma E_z)$ and $B_\phi \equiv 0$ which is a result of the symmetry, and of the absence of current sources inside the tube. Equations (3), (4) and (5) constitute the boundary and initial conditions of the problem.

The solution may be obtained by means of the Laplace transform. Accordingly, with $\mathcal{L}\left\{i_z(x,y)\right\} \equiv \bar{i}(x,p)$,

$$\bar{i}(x,p) = \int_0^\infty i_z(x,y) \, e^{-py} dy \quad , \tag{6}$$

and Eq. (2) becomes

$$\frac{\partial^2 \bar{i}(x,p)}{\partial x^2} + \frac{1}{x} \frac{\partial \bar{i}(x,p)}{\partial x} - p\bar{i}(x,p) = 0 \quad , \tag{7}$$

9

with solution

$$\bar{i}(x,p) = A(p)\, I_0(p^{1/2}x) \;+\; B(p)\, K_0(p^{1/2}x) \tag{8}$$

where I_0 and K_0 are modified Bessel functions of the first and second kind for imaginary argument.[9] The functions $A(p)$ and $B(p)$ can be obtained from the boundary conditions (3) and (6) after one takes the Laplace transform of these equations under the assumption that the order of operations can be interchanged. The result is

$$\bar{i}(x,p) = \frac{\mathcal{L}\{\mathcal{U}(q)\}}{2\pi a^2}\;\; \frac{\left[K_0'(\epsilon p^{1/2})\, I_0(xp^{1/2}) - I_0'(\epsilon p^{1/2})\, K_0(xp^{1/2})\right]}{\left[K_0'(\epsilon p^{1/2})\displaystyle\int_\epsilon^1 I_0(xp^{1/2})\, x\,dx - I_0'(\epsilon p^{1/2})\displaystyle\int_\epsilon^1 K_0(xp^{1/2})\, x\,dx\right]} \tag{9}$$

where primes indicate differentiation with respect to the argument. The desired current function, $i_z(x,y)$, can now be found using the inversion integral theorem. Keeping Eq. (9) in view we write

$$i_z(x,y) = \frac{1}{2\pi i}\; \lim_{\beta \to \infty}\; \int_{\alpha - i\beta}^{\alpha + i\beta} e^{yp}\, \bar{i}(x,p)\; dp\;\; , \tag{10}$$

where α lies to the right of all of the singularities of $\bar{i}(x,p)$. The task of exhibiting the function $i_z(x,y)$, once the Laplace transform of the applied total current $\mathcal{U}(y)$ has been determined, is now seen to be that of evaluating the open contour integral (10). If the singularities of the integrand are simple poles, then a well known expansion theorem allows expression of $i_z(x,y)$ as the sum of the residues of the integrand. This is the form in which Haines gives the exact solution to the skin effect problem for a solid cylindrical conductor. No equivalent exact solution has been found for the tubular conductor represented by Eq. (10). A partial investigation of the poles of Eq. (9) shows that there are none in the immediate vicinity of the origin. With the aid of the definitions

10

and recurrence relations among the Bessel functions the denominator of
Eq. (9) can be transformed.into a more familiar form (see Eq. (28) below)
whose first few zeros are tabulated in Jahnke and Emde.[10] These
identify the first members of a denumerable infinity of poles of the
integrand on the negative real axis. Additional values can be
calculated from the appropriate asymptotic expansions for the Bessel
functions. While the values of the real, negative poles can be
determined to sufficient accuracy, convenient analytical expressions
for the residues have not been obtained; furthermore, no proof is at
hand excluding the possibility of complex poles of the denominator in
the left half plane. Because of these lacks the exact solution for
$i_z(x,y)$ cannot be written down in explicit form convenient for
calculation. While it is reasonable to suppose that these gaps in
the analysis can eventually be closed, the difficulties are formidable
and make a more accessible, approximate method seem preferable for the
present. Accordingly we proceed now with the development of such a
method.

2.2 Approximate Solution

An appropriate simplification can be found by examining Eq. (7) and
recalling that in order to minimize skin effect the tubular shunt must
be thin. This means that the variation of $x(= r/a)$ is typically limited
to the range $0.9 \doteq \epsilon \leq x \doteq 1.0$, and in the case with which we are
principally concerned the ratio ϵ of inner to outer radius of the shunt
is 0.93. Ideally the measuring element of the shunt should be as thin
as possible, but the necessity to resist the self pinch forces of the
current requires greater wall thickness than is strictly needed for
electrical reasons alone.

With this limitation on x we see that the coefficient $1/x$ in Eq. (7)
could reasonably be replaced by $1/x_m$ where $\epsilon < x_m < 1$.[*] Once this is

---

[*] The possibility of this simplification was pointed out to the author
by Mr. J. E. Hunsicker of this laboratory.

11

done the approximate solution for transformed current is

$$\bar{\imath}(x,p) = A_1(p)\, e^{f_1 x} \;+\; B_1(p)\, e^{f_2 x} \quad , \tag{11}$$

where

$$\binom{f_1}{f_2} = -\frac{1}{2x_m} \;\pm\; \sqrt{\frac{1}{4x_m^2} + p} \tag{12}$$

and x_m is taken to be $(1 + \epsilon)/2$. Using the boundary conditions to evaluate A_1 and B_1 we obtain

$$\bar{\imath}(x,p) = \frac{\mathcal{L}\left\{\mathcal{U}(q)\right\}}{2\pi a^2}\;\frac{\left[f_2 e^{f_1(x-\epsilon)} - f_1 e^{f_2(x-\epsilon)}\right]}{\displaystyle\int_\epsilon^1 \left[f_2 e^{f_1(\xi-\epsilon)} - f_1 e^{f_2(\xi-\epsilon)}\right]\,\xi\,d\xi}\,. \tag{13}$$

While Eq. (13) is analytically much more transparent than its counterpart Eq. (9), evaluating the inversion integral is still far from simple. We carry the approximation procedure two steps further.

First, we replace ξ in the integrals of Eq. (13) by the mean value $x_m = (1 + \epsilon)/2$; and second, after integration, approximate the resulting exponentials by their series expansions, retaining terms up to fifth degree in the arguments to ensure sufficient accuracy. The choice for x_m may be justified by noting from Eq. (3) that when current is assumed constant over the cross section, the area S is given by product of mean circumference with thickness in the form $S = 2\pi a \left[(1 + \epsilon)/2\right]\left[a(1 - \epsilon)\right]$, from which we identify x_m as the dimensionless mean radius.

After the integration we have

$$\bar{\imath}(x,p) = \frac{\mathcal{L}\left\{\mathcal{U}(q)\right\}}{2\pi a^2 x_m}\;\frac{f_1 f_2 \left[f_2 e^{f_1(x-\epsilon)} - f_1 e^{f_2(x-\epsilon)}\right]}{\left[f_2^2\left(e^{f_1(1-\epsilon)} - 1\right) - f_1^2\left(e^{f_2(1-\epsilon)} - 1\right)\right]}\quad , \tag{14}$$

12

and upon expanding the exponentials, keeping Equation (12) in mind,

$$\bar{i}(x,p) = \frac{\mathcal{L}\{\mathcal{L}(q)\}}{2\pi a^2 x_m (1 - \epsilon)} \frac{\left\{1 + \left[p(x - \epsilon)^2/2\right]\left[1 - (x - \epsilon)/3x_m \cdots\right]\right\}}{\left\{1 + \left[p(1 - \epsilon)^2/6\right]\left[1 - (1 - \epsilon)/4x_m + (1 - \epsilon)^2/20x_m^2 \cdots\right]\right\}}.$$

(15)

Notice here that the denominator of the first factor is just the area S of the tube cross section; and that, aside from those introduced by the transform of the impressed current $\mathcal{L}(y)$, there is only one pole; and it is located on the negative real axis. It is completely determined by the thickness and mean radius of the tube.

2.3 Current Response of the Tubular Shunt

We can further specialize Eq. (15) by setting $x = \epsilon$, thereby obtaining only the transformed current density at the inner radius where the sensing probe is located. This is all we need for comparison of the shunt response with the arbitrary impressed current.

Suppose that impressed current is taken to be a damped sine wave of unit amplitude, i.e., $\mathcal{L}(y) = e^{-\alpha y} \sin \omega y$. Then $\mathcal{L}\{\mathcal{L}(q)\} = \omega/\left[(p+\alpha)^2 + \omega^2\right]$ and the Laplace transform of $\mathcal{L}$ introduces two poles into Eq. (15) in addition to the one already found. When the inverse transform is taken, three terms will be obtained, one corresponding to each pole, and two will be steady state terms from the impressed current. The third will be a transient term arising from the denominator of Eq. (15). Whereas the poles, and corresponding transient terms of the exact solution Eq. (9), are at least denumerably infinite; the approximations by which Fq. (15) is obtained reduce this infinity to one. Accordingly only one transient term is to be expected in the expression for true current; however, this transient may be regarded as fairly typical of the infinity of terms in the exact solution. Note that because of our choice of the variable y it follows that $\alpha = \alpha' \mu\sigma a^2$ and $\omega = \omega' \mu\sigma a^2$ where $\alpha' = R/2L$ and $\omega' = (1/LC - R^2/4L^2)^{1/2}$ in terms of the known circuit constants.

13

Under the above conditions Eq. (15) is now simplified enough
so that an inverse transformation can easily be found. It is

$$
i_z(\epsilon,y) = \frac{\omega/\gamma}{S\left[(1 - \alpha/\gamma)^2 + (\omega/\gamma)^2\right]} \left[e^{-\gamma y} + (\gamma/\omega)(1 - \alpha/\gamma) e^{-\alpha y} \sin \omega y - e^{-\alpha y} \cos \omega y\right],
$$

(16)

where
$$
\gamma = \left[6/(1 - \epsilon)^2\right] \left[1 - (1 - \epsilon)/4x_m + (1 - \epsilon)^2/20x_m\right]^{-1} .
$$

At the origin of time $y = 0$ and $i_z(\epsilon,0) = 0$.

The quantity $S\, i_z(\epsilon,y)$ is the total apparent current as reported
by the shunt on the assumption that the current density at $x = \epsilon$ is
constant over the entire cross section. This apparent current is just
the quantity we wish to compare with the impressed current $\mathcal{U}(y)$.
Certain general conclusions can be reached by further analysis of
Eq. (16).

If the shunt thickness approaches zero, then $\epsilon \rightarrow 1$ and the pole - γ
takes on a negative value as large as we please. The first and third
terms of (16) are negligible and we recover exactly the impressed
current $e^{-\alpha y} \sin \omega y$. Therefore the approximate treatment predicts
that a sufficiently thin shunt will measure the impressed current as
accurately as desired.

Under slightly less restrictive conditions, if $\omega \ll \gamma$ and $1 - \alpha/\gamma$
is of order unity, the first and third terms have coefficients much
smaller than the dominating central term. Near current peak $\sin \omega y \approx 1$
and the first and third terms may be neglected. The amplitude
of the $\sin \omega y$ term is, to good approximation, just $1 + \alpha/\gamma$; so an
estimate of accuracy of the peak current reading can be made. In
the examples of interest it is also true that $\alpha \ll \gamma$ and magnitude
of expected error in the current peak is less than 1%.

14

2.4 Initial Current Slope

To examine the initial current rise sensed by the shunt we need expressions for the first and second derivatives of Eq. (16). With the definition $I_s = S\, i_z(\epsilon, y)$, these may be written as

$$\frac{dI_s}{dy} = \frac{\omega e^{-\alpha y}}{(1 - \alpha/\gamma)^2 + (\omega/\gamma)^2}\left[\cos \omega y - e^{-(\gamma - \alpha)y} + (\omega/\gamma - \alpha/\omega + \alpha^2/\omega\gamma)\,\sin \omega y\right], \tag{17}$$

and

$$\frac{d^2 I_s}{dy^2} = \frac{\omega e^{-\alpha y}}{(1 - \alpha/\gamma)^2 + (\omega/\gamma)^2}\left[(\omega/\gamma - 2\alpha/\omega + \alpha^2/\gamma\omega)\,\omega \cos \omega y + \gamma e^{-(\gamma - \alpha)y}\right.$$
$$\left. - (1 + \alpha/\gamma - \alpha^2/\omega^2 + \alpha^3/\omega^2\gamma)\,\omega \sin \omega y\right]. \tag{18}$$

From Eq. (17) it is clear that when $y = 0$ the first derivative vanishes; so, regardless of thickness, the shunt reports initial slope as zero, in contrast to the positive value ω for the impressed current. While the slope of the impressed current falls monotonically to zero in the first quarter-cycle, the slope measured by the shunt must rise to some maximum value and then decrease. This maximum is necessarily less than ω, although for the class of thin shunts, in which we are mainly interested, the difference is only a few percent. The argument proceeds as follows.

The maximum of slope will occur where the second derivative, Eq. (18), vanishes; thus the bracket on the right must be zero. Since this must occur while $\omega y \lesssim 1/4$, i.e., quite early in the cycle if the shunt is to reproduce the wave form at all accurately, we can approximate the trigonometric terms by 1 and ωy respectively. If $\alpha < \omega \ll \gamma$, the condition reduces to

$$(\omega/\gamma - 2\alpha/\omega)\,\omega/\gamma - (\omega/\gamma)^2\,\gamma y + e^{-\gamma y} = 0 \quad, \tag{19}$$

15

from which an approximate solution can be readily found. Given the solution as $y = y_1$, Eq. (19) and the inequalities can be used to simplify the expression for the maximum slope sensed by the shunt. The result is

$$\left[\frac{dI_s}{dy}\right]_{max} \doteq \omega \left[1 - \alpha y_1 - 2\alpha/\gamma\right] , \tag{20}$$

and we see that, to this approximation, the indicated maximum slope is always less than that of the impressed current.

2.5 Typical Cases

In Table I values are given for two nichrome, shunts used for current measurements in the recent series of exploding wire experiments.[6] The sensing element of the shunt in each case had an outer radius $a = 3.175 \times 10^{-3}$m, conductivity $\sigma = 0.926 \times 10^6$ mho/m,

TABLE I

	ϵ	α	ω	γ	γy_1	$1 + \alpha/\gamma$	$\left[1-(\alpha/\gamma)(\gamma y_1+2)\right]$
Shunt I	.926	3.495	32.84	1117.	4.664	1.003	0.979
Shunt II	.880	Same	Same	430.1	3.483	1.008	0.956

and the time scaling factor $\mu\sigma a^2 = 11.72$ μsec. The last two columns show the deviations in peak current and initial slope, respectively, to be expected on account of the transient skin effect.

Measurements of initial current slopes from experimental records provided by the shunts may yield values less by several percent than the estimates given in the last column of Table I. In the practical case, an average is taken, graphically or analytically, among measured slopes near the origin of time. Because of the characteristic response of the tubular shunt given by Eq.(16) - (18), values of slope less than the maximum will predominate and the experimentally determined value must necessarily be less than the true maximum the shunt can indicate. Slope discrepancies up to 10% may conceivably be accounted for in this way.

16

If the experimenter weights the limiting slope value at the apparent origin in time most heavily, under the impression that the maximum slope will appear when $t = y = 0$, then a value may be obtained even more in error than if he gives equal weight to all early slopes. Failure of the oscilloscope to follow accurately the rise of shunt voltage will introduce an additional factor tending to produce too low an initial slope.

In making the preceding estimates it is presumed that the scaling factor $\mu\sigma a^2$ is accurately known, but an unsuspected error in its value would have a proportionate effect in the values of α and ω without changing the value of γ. While radius $\underline{a}$ is easily determined to within 1%, finding the appropriate values of μ and σ for high, current-rate pulses presents much greater difficulty. Increases in α and ω corresponding to an increase in μ, say, will tend to reduce the value of γy_1, but not as rapidly as the ratio α/γ increases, and increase both the deviation in peak current and the lowering of initial slope from the expected values.

In concluding this section we repeat again that transient skin effects will necessarily cause a tubular current shunt to report low values of initial current rise and the error may be 10% or larger.

17

TRANSIENT RESISTANCE OF CIRCUIT ELEMENTS

From the nature of the diffusion of an electromagnetic wave into a conductor, it is intuitively clear that the initial resistance of such a conductor must be infinite at the time of incidence of the wave. Thereafter the resistance falls rapidly to the value characteristic of the ordinary skin effect in the case of a continuous oscillation or to the d.c. value if no oscillation is involved. The question arises under what conditions, if any, can this transient, excess resistance seriously alter the initial conditions determining a damped oscillation. Simple calculations with the damped sine wave formula indicate that if the circuit resistance is larger than its steady state value by a factor of 2.5 in the first quarter-cycle, the first current peak will be too low by 25%. It follows that higher average resistance over a shorter time interval can accomplish the same result. Interest then focuses on the exact form of time dependence of the transient resistance; for a resistance varying hyperbolically with time as current increases linearly, can produce a finite RI drop at t = 0 and thus alter the initial conditions under which a damped oscillation would commence and in particular reduce the initial current slope.

Since most of the resistance of a typical discharge circuit is concentrated in the condenser bank, we shall examine the resistance variation of an ideal flat plate condenser with respect to transient skin effect and provide estimates of the change in initial conditions which may occur from this cause. The treatment will consist in solution of the flat plate condenser problem and use of the asymptotic solution, valid near the origin in time, to compute numerically the resistance variation of a condenser similar in some respects to those actually employed. It will also be shown that the asymptotic solutions for the solid-cylindrical and cylindrical-tube conductors are identical in functional form with that for the flat plate; so that similar behavior can be expected for connecting wires, spark terminals, etc. which have cylindrical symmetry. On account of the comparatively large dimensions of these elements their contribution to the total resistance is small and may be considered negligible.

16

3.1 Flat Plate Condenser - Asymptotic Solution

We seek the current distribution in an infinite flat plate of thickness $\underline{a}$ representing one-half of a parallel plate condenser. Assume rectangular coordinates with x' in the direction transverse to the plate and z' in the direction of current flow. As before, x and y are dimensionless space and time variables such that $x = x'/a$ and $y = t/\mu\sigma a^2$ with $0 \leq x \leq 1$. The entire formulation given in § 2.1 may be paraphrased and the analysis carried through in detail. The analog of Eq. (5) in terms of $i_z(x,y)$ (where $z \equiv z'$) can be written as $\left[\partial i_z/\partial x\right]_{x=1} = 0$. In order for the total current, $\mathcal{Cl}$, to remain finite it is necessary to consider a finite portion of the plate of width w. One finds without difficulty that

$$\bar{i}(x,p) = \frac{\sqrt{p}\ \cosh\left[\sqrt{p}(1-x)\right]\ \mathcal{L}\left\{\mathcal{Cl}(q)\right\}}{wa\ \sinh\sqrt{p}} \quad . \tag{21}$$

We investigate the asymptotic representation of this solution, and its inverse transform, for large p corresponding to small values of y. If p is sufficiently large the Laplace transforms of any of the following: current ramp, sine wave or damped sine wave are all the same, viz.,

$$\mathcal{L}\left\{\begin{array}{l} \omega q \\ \sin \omega q \\ e^{-\alpha q}\sin \omega q \end{array}\right\} \sim \omega/p^2 \quad , \tag{22}$$

and we take the condition for the validity of (22) to be $p \gg \omega > \alpha$, an inequality which has already arisen in connection with the approximate solution. If $\sqrt{p}\ (1-x) > 2.5$ and to avoid an infinite p we take $x < 1$, i.e., x is bounded away from 1, the hyperbolic functions in Eq. (21) can be replaced to an accuracy of about 1% by their leading exponential terms. Thus

$$\bar{i}(x,p) \sim \frac{\omega}{wa}\ \frac{e^{-\sqrt{p}x}}{p^{3/2}} \tag{23}.$$

19

with $\sqrt{p} > 2.5/(1 - x)$ (23a)

and $p \gg \omega > \alpha$.   (23b)

While in the analysis up to Eq. (23), p is considered real and
positive, when the inversion is considered via contour integral
Eq. (10), the analytic continuation of Eq. (23) throughout the
entire complex plane is involved. A branch point is seen to exist
at p = 0 and the inverse is found by integrating along both sides of
a contour which when shrunk coincides with the negative real axis.[*]
To estimate the upper limit on $y > 0$ for which the asymptotic solution
might be valid, we observe that the exponential in Eq. (10) will damp
out any contribution to the integral occurring along the negative real
axis save in the range $0 \leq |yp| \leq 1$. The upper limit of order unity
is somewhat arbitrary, but would probably never be chosen larger than
5. Thus we expect the asymptotic solution to be valid for $|p|$ large
and $0 \leq y < 1/|p|$. The inequalities (23a) and (23b), or equivalent ex-
pressions, serve to define the smallest permitted magnitude of p and
therefore the largest permitted value of y.

With these conditions in mind we now quote the inverse of Eq. (23)
from a table of transforms. The inverse is

$$i_z(x,y) \sim (\omega/wa) \; \left[2\sqrt{y/\pi} \; \exp(-x^2/4y) - x \; \mathrm{erfc} \; (x/2\sqrt{y}) \right. , \; (24)$$

where

$$\mathrm{erfc} \; (x) = 1 - \mathrm{erf} \; (x) = (2/\sqrt{\pi}) \int_x^{\infty} e^{-\xi^2} d\xi \; .$$

---

* Cf. the discussion given by Carslaw and Jaeger, Conduction of Heat
in Solids 2nd Ed., (Oxford University Press, 1959) pp 302-303 and
Appendix I.

An alternate form is

$$i_z(x,y) = (\omega/wa) \int_0^y \frac{\exp\ (-\ x^2/4\xi)\ d\xi}{\sqrt{\pi\xi}} \quad . \tag{24a}$$

We note in passing that if $x \neq 0$, i_z and all of its derivatives with respect to y vanish at $y = 0$ because of the singularity of the function at this point.

3.2 Resistance Variation with Time

To find the time dependent resistance of the flat plate we calculate the electrical power dissipated in a section of length ℓ and width $\underline{w}$. With the help of Ohm's law and the current density i_z we find

$$P(y) = (\ell wa/\sigma) \int_0^1 i_z^2 (x,y)\ dx \quad . \tag{25}$$

We may also express the power as product of instantaneous resistance times total current squared. Thus

$$P(y) = R(y)\ I^2(y)$$
$$= R(y) \left[wa \int_0^1 i_z (x,y)\ dx \right]^2 \quad . \tag{26}$$

Equating Eq. (25) and (26) and using $R_{dc} = \ell/\sigma wa$ leads to

$$R(y)/R_{dc} = \int_0^1 i_z^2 (x,y)\ dx \bigg/ \left[\int_0^1 i_z (x,y)\ dx \right]^2 \quad , \tag{27}$$

an expression that is free of the dimensions of the plate. For this reason it can be taken as representative of the resistance variation of the entire condenser.

21

Using Eqs. (24) and (27), numerical calculations have been made
for an aluminum, flat plate condenser with plate thickness
$a = 1.4 \times 10^{-5}$m, the same as that of the foil in the condensers
actually employed. For aluminum, $\sigma = 3.7 \times 10^7$ mho/m and $\mu\sigma a^2 = 9.1 \times 10^{-9}$
sec. In the exploding wire studies previously mentioned[6] the basic
frequency is 0.446 mc and the appropriate value of ω is .0255. If
we adopt this value of ω as representative, it is clear that any
value of p larger than unity will satisfy inequality (23b) quite well.

On the other hand (23a) imposes a much more severe restriction on
values of p and y. For example if $x \leq 0.5$ the requirement (23a) demands
$p > 25$ and the relevant interval of y is $0 \leq y \leq .04$ which corresponds to a
time interval of less than 1/2 nano-sec. It might be thought that
integrating over the range $0 \leq x \leq 1$ in Eq. (27) would involve such an
inaccurate representation of i_z in the neighborhood of $x = 1$ that the
calculation would be vitiated. Such is not the case; because, for these
early times $(y \leq .04)$, the current is concentrated mainly in the region
$x \leq 0.5$ and the contribution to the integrals from the remainder of the
range is typically a few tenths of a percent and in the worst case less
than 4%. The calculations show that, in this range of y values
$2.8 \leq R(y)/R_{dc} \leq 23.4$, i.e., transient resistance falls steeply from
infinity to about three times the dc value in 1/2 nano-sec. In this
interval the resistance variation is represented within about 5% by
the relation $R(y)/R_{dc} = 1 + 0.377/y^{0.644}$.

The significance of this result lies in the implication that for
a current increase linear with time and consequently linear with y,
the limit as $y \rightarrow 0$ of $R(y)$ i (y) is zero. Thus the Ri term in the
circuit equation for a damped oscillation has no limiting value other
than zero and cannot influence the initial rise of current. For this
reason, we can eliminate the transient condenser resistance as a
possible cause of a slope discrepancy at $t = 0$. Furthermore, the
fall from infinite resistance to values comparable with the steady state
resistance occurs in a small fraction of the first quarter-cycle. This

22

calculation shows $R(y)/R_{dc} < 1.1$ by $t = 9.1$ nano-sec. which interval
is only 2% of the first quarter-cycle. Therefore, while the
calculation for $y > .04$ is admittedly of problematic accuracy because
the limiting inequalities (23a) and (23b) are no longer satisfied,
the indications are strong that transient resistance cannot contribute
any appreciable deviations from the expected damped-sine-wave behavior
of the circuit.

3.3 Asymptotic Solutions - Cylindrical Geometry

We complete our discussion by indicating here the form of the
asymptotic solutions characteristic of the tubular current shunt and of
the solid cylindrical conductor. We outline the procedure omitting
details.

Starting from Eq. (9) and making use of differential relations
among the I's and K's,[5] one obtains

$$\bar{i}(x,p) = \frac{\alpha\left\{\mathcal{U}(q)\right\}}{2\pi a^2} \; \frac{\sqrt{p}\left[K_1(\epsilon\sqrt{p})\,I_0(x\sqrt{p}) + I_1(\epsilon\sqrt{p})\,K_0(x\sqrt{p})\right]}{\left[I_1(\sqrt{p})\,K_1(\epsilon\sqrt{p}) - I_1(\epsilon\sqrt{p})\,K_1(\sqrt{p})\right]} \quad .$$

$$(28)$$

Then with the asymptotic expressions for the Bessel functions with
arguments greater than 10 (Cf. ref. 5 pp. 220-221), using Eq. (22)
and dropping all but the leading terms, Eq. (28) simplifies, with
an accuracy better than 3%, to

$$\bar{i}(x,p) \sim \frac{\omega}{2\pi a^2 \sqrt{x}} \; \frac{\cosh\sqrt{p}(x - \epsilon)}{p^{3/2}\sinh\sqrt{p}(1 - \epsilon)} \quad , \tag{29}$$

under the restrictions that

$$\sqrt{p} > 2.5/(1 - \epsilon) \tag{29a}$$

and $p > 10\omega > \alpha$. $\tag{29b}$

23

If the inequality $\sqrt{p}(x - \epsilon) > 2.5$ can be maintained, then we can write

$$\bar{i}(x,p) \sim \frac{\omega}{2\pi a^2 \sqrt{x}} \quad \frac{e^{-\sqrt{p}(1 - x)}}{p^{3/2}} \quad , \tag{30}$$

and the close analogy with Eqs. (23), (23a) and (23b) is immediately seen. As before, an infinity of p will occur to preserve the inequality in the neighborhood of $x = \epsilon$; but, as in the previous case, the transformed current distribution will be least in the immediate vicinity of the critical value $x = \epsilon$, with the probable result that integrals for current and power will be only slightly affected by the inaccurate representation offered by (30).

In a similar way we can show without difficulty that the asymptotic form for the cylindrical conductor obtained from Haines' Eq. (11),[3] is exactly Eq. (30) where inequality $\sqrt{p} > 12.5 \, (1/x + 3)$ must hold if 1% accuracy is desired. For this case $x > 0$ is required to preserve the inequality, but the usual arguments may be given for using the transformed asymptotic current in calculations of current and power. In cylindrical coordinates these integrals will contain an additional factor of x, but the behavior of the integrand will be dominated by the function given in Eq. (24). We may then state with confidence that the transient skin-effect resistance in all three cases, viz., planar, cylindrical and tubular will follow similar laws. We may draw the conclusion that no adverse effect on initial conditions in oscillatory exploding wire circuits is to be expected from transient skin effect in condenser, shunt or lead wires. These conclusions only hold when the characteristic time, $\mu\sigma a^2$, is negligible compared with the time of one oscillation. Should these times become the same within an order of magnitude, then we may expect appreciable and important effects to arise from the dissipation caused by the transient skin effect resistance.

F. D. Bennett

F. D. BENNETT

24

REFERENCES

1. Park, J. H.   J. Research Nat'l. Bur. Standards $\underline{39}$, 191 (1947).

2. Durnford, J. and Reynolds, P. Proc. Inst. Elect. Engrs. IV, $\underline{101}$, 1-6 (1954).

3. Barrington, A. E.   Brit. J. Appl. Phys. $\underline{7}$, 408 (1956).

4. Chace, W. G., Morgan, R. L. and Saari, K. P. Exploding Wires (Plenum Press, Inc. New York, 1959) p. 59.

5. Ripoche, J. phys. radium. Suppl. No. 2, $\underline{22}$, 48A (1961).

6. Bennett, F. D., Burden, H. S. and Shear, D. D. Correlated Electrical and Optical Measurements of Exploding Wires. BRL Report No. 1133 (1961) also Phys. of Fluids, in press.

7. Haines, M. G.   Proc. Phys. Soc. $\underline{74}$, 576 (1959).

8. Maninger, R. C. Exploding Wires, Edited by W. G. Chace and H. K. Moore (Plenum Press, New York, 1959) p. 156.

9. McLachlan, N. W. Bessel Functions for Engineers (Oxford University Press, 2nd Ed. 1955) pp. 190, 200, 203, 204.

10. Tables of Functions, (Reprint by Dover Publications, New York 1943) pp. 204 - 206.

CURRENT TERMINALS

OUTER CURRENT-CONDUCTOR

INNER CURRENT-CONDUCTOR

NICHROME-V RESISTANCE ELEMENT

OUTER MEASUREMENT-LEAD

INNER MEASUREMENT-LEAD
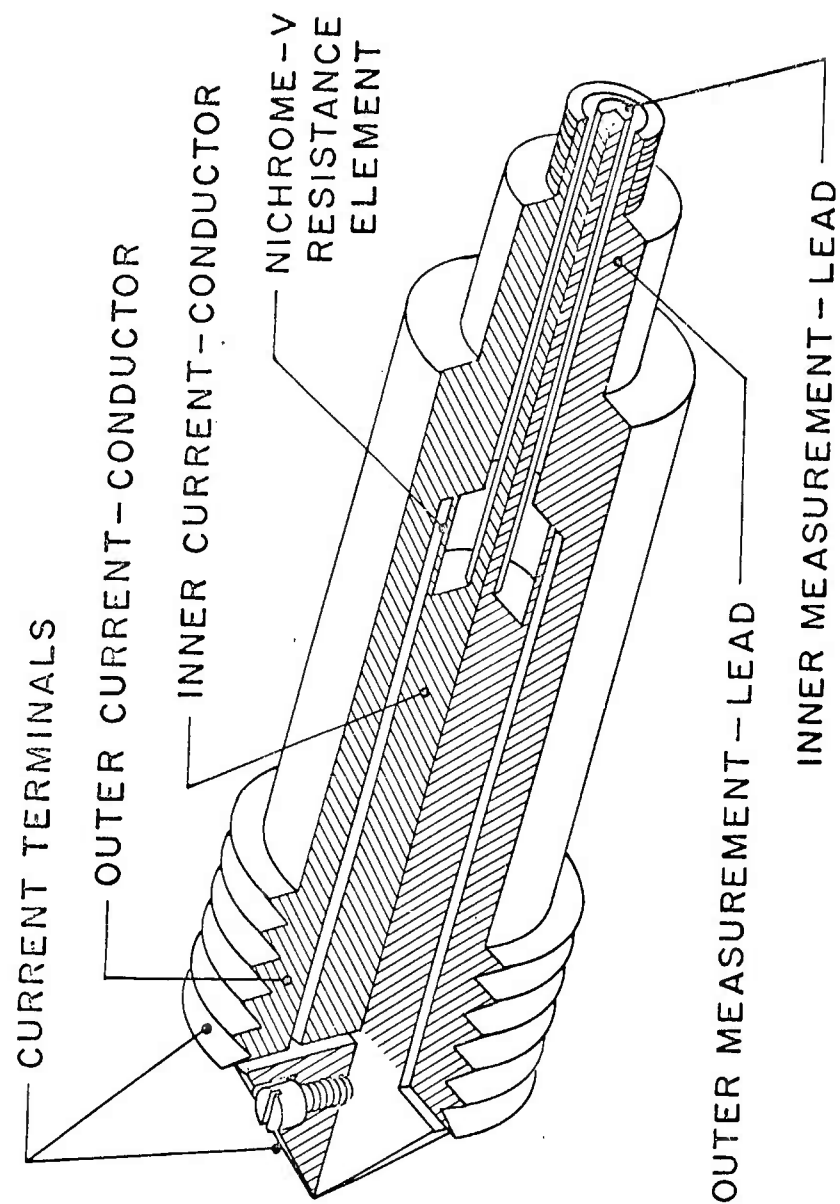
Fig. 1   Current Measuring Resistance

DISTRIBUTION LIST

No. of Copies	Organization	No. of Copies	Organization
2	Chief of Ordnance ATTN: ORDTB - Bal Sec ORDTN Department of the Army Washington 25, D. C.	1	Superintendent U. S. Naval Postgraduate School Monterey, California
1	Commanding Officer Diamond Ordnance Fuze Laboratories ATTN: Technical Information Office Branch 012 Washington 25, D. C.	1	Director U. S. Naval Research Laboratory ATTN: Dr. A. C. Kolb Washington 25, D. C.
		1	Commander U. S. Naval Weapons Laboratory Dahlgren, Virginia
10	Commander Armed Services Technical Information Agency ATTN: TIPCR Arlington Hall Station Arlington 12, Virginia	1	Commander Air Proving Ground Center ATTN: PGAPI Eglin Air Force Base, Florida Of Interest to: PGEM
10	Commander British Army Staff British Defence Staff (W) ATTN: Reports Officer 3100 Massachusetts Avenue, NW Washington 8, D. C.	3	Commander Air Force Cambridge Research Laboratory ATTN: W. G. Chace - CRZN M. A. Levine M. O'Day L. G. Hanscom Field Bedford, Massachusetts
4	Defence Research Member Canadian Joint Staff 2450 Massachusetts Avenue, NW Washington 8, D. C.	1	Commander Air Force Special Weapons Center ATTN: SWRP Kirtland Air Force Base, New Mexico
3	Chief, Bureau of Naval Weapons ATTN: DIS-33 Department of the Navy Washington 25, D. C.	1	Director Air University Library ATTN: AUL (3T-AUL-60-118) Maxwell Air Force Base, Alabama
1	Commander Naval Ordnance Laboratory ATTN: Library White Oak, Silver Spring 19, Maryland	1	Commander Aeronautical Systems Division ATTN: WWAD Wright-Patterson Air Force Base, Ohio
1	Commander U. S. Naval Ordnance Test Station ATTN: Technical Library China Lake, California	2	Commanding General Frankford Arsenal ATTN: Mr. Charles Lukens, Bldg. 150 Library Branch, 0270, Bldg. 40 Philadelphia 37, Pennsylvania

DISTRIBUTION LIST

No. of Copies	Organization	No. of Copies	Organization
3	Commanding Officer Picatinny Arsenal ATTN: Feltman Research and Engineering Laboratories NASL Mr. S. S. Verner Dover, New Jersey	1	Director National Aeronautics and Space Administration Langley Research Center Langley Field, Virginia
1	Commanding General Army Ballistic Missile Agency ATTN: Dr. T. A. Barr Redstone Arsenal, Alabama	1	Director National Aeronautics and Space Administration Lewis Research Center Cleveland Airport Cleveland, Ohio
1	Commanding General Army Rocket & Guided Missile Agency ATTN: Supporting Research Branch Redstone Arsenal, Alabama	1	Director National Bureau of Standards ATTN: Mr. Paul H. Krupenie 232 Dynamometer Building Washington 25, D. C.
1	Army Research Office Arlington Hall Station Arlington, Virginia	1	U. S. Atomic Energy Commission ATTN: Technical Reports Library Mrs. J. O'Leary for Division of Military Applications Washington 25, D. C.
1	Applied Physics Laboratory The Johns Hopkins University 8621 Georgia Avenue Silver Spring, Maryland	3	U. S. Atomic Energy Commission Los Alamos Scientific Laboratory ATTN: Dr. J. L. Tuck Dr. R. G. Schreffler Dr. R. E. Duff P. O. Box 1663 Los Alamos, New Mexico
1	Jet Propulsion Laboratory ATTN: Mr. Irl E. Newlan - Reports Group 4800 Oak Grove Drive Pasadena, California		
1	Director National Aeronautics and Space Administration 1520 H Street, NW Washington 25, D. C.	1	Cornell Aeronautical Laboratory, Inc. ATTN: Mr. Joseph Desmond - Librarian 4455 Genessee Street Buffalo 5, New York
2	Director National Aeronautics and Space Administration Ames Research Center ATTN: Mr. V. J. Stevens Mr. Harvey Allen Moffett Field, California	1	Datamatic Corporation ATTN: Dr. R. F. Clippinger 151 Needham Street Newton Highlands 61, Massachusetts

DISTRIBUTION LIST

No. of Copies	Organization	No. of Copies	Organization
2	General Electric Research Laboratory ATTN: Dr. R. A. Alpher Dr. D. R. White P. O. Box 1088 Schenectady, New York	1	Pennsylvania State University Physics Department ATTN: Professor R. G. Stoner State College, Pennsylvania
1	California Institute of Technology Aeronautics Department ATTN: Professor H. W. Liepmann 1201 East California Street Pasadena 4, California	1	Princeton University James Forrestal Research Center ATTN: Professor S. Bogdonoff Princeton, New Jersey
1	California Institute of Technology Guggenheim Aeronautical Laboratory ATTN: Professor L. Lees Pasadena 4, California	1	Princeton University Observatory ATTN: Professor Lyman Spitzer, Jr. Princeton, New Jersey
1	Case Institute of Technology Department of Mechanical Engineering ATTN: Professor G. Kuerti University Circle Cleveland 6, Ohio	1	Stanford University Department of Mechanical Engineering ATTN: Professor D. Bershader Stanford, California
1	Cornell University Graduate School of Aeronautical Engineering ATTN: Professor E. L. Resler Ithaca, New York	1	Syracuse University Department of Physics ATTN: Professor C. H. Bachman Syracuse, New York
1	Harvard Observatory Harvard University ATTN: Professor F. L. Whipple Cambridge 38, Massachusetts	1	University of California Low Pressures Research Project ATTN: Professor S. A. Schaaf Berkeley 4, California
1	The Johns Hopkins University Department of Aeronautics ATTN: Professor L. S. G. Kovaszny Baltimore 18, Maryland	1	University of Chicago The Enrico Fermi Institute of Nuclear Studies ATTN: Professor E. N. Parker Chicago 37, Illinois
1	Lehigh University Department of Physics ATTN: Professor R. J. Emrich Bethlehem, Pennsylvania	1	University of Illinois Aeronautical Institute ATTN: Professor B. L. Hicks Urbana, Illinois
		2	University of Maryland Institute for Fluid Dynamics and Applied Mathematics ATTN: Professor S. I. Pai Professor J. M. Burgers College Park, Maryland

DISTRIBUTION LIST

No. of Copies	Organization	No. of Copies	Organization
1	University of Michigan Department of Physics ATTN: Professor Otto Laporte Ann Arbor, Michigan	1	Professor J. Lloyd Bohn Temple University Department of Physics Philadelphia, Pennsylvania
1	University of Michigan Willow Run Laboratories P. O. Box 2008 Ann Arbor, Michigan	1	Professor R. G. Campbell Hartford Graduate Center R.P.I. East Windsor Hill, Connecticut
1	University of Oklahoma Department of Physics ATTN: Professor R. G. Fowler Norman, Oklahoma	1	Mr. Paul R. Caron - Research Assistant Brown University Engineering Division Providence, Rhode Island
1	University of Pennsylvania Moore School of Electrical Engineering ATTN: Professor S. Gorn Philadelphia, Pennsylvania	1	Professor G. F. Carrier Division of Engineering and Applied Physics Harvard University Cambridge 38, Massachusetts
1	Dr. G. W. Anderson Sandia Corporation Sandia Base P. O. Box 5800 Albuquerque, New Mexico	1	Dr. Eugene C. Cnare Sandia Corporation Sandia Base P. O. Box 5800 Albuquerque, New Mexico
1	Professor J. W. Beams University of Virginia Department of Physics McCormic Road Charlottesville, Virginia	1	Mr. Robert Dennen Armour Research Foundation Illinois Institute of Technology Center Chicago, Illinois
1	Professor R. C. Binder University of Southern California Engineer Center University Park Los Angeles 7, California	1	Mr. Robert W. Ellison Director, Research & Engineering National Electronics Laboratories, Inc. 1713 Kalorama Road, NW Washington 9, D. C.
1	Professor W. Bleakney Princeton University Palmer Physical Laboratory Princeton, New Jersey	1	Professor H. W. Emmons Harvard University Cambridge 38, Massachusetts

DISTRIBUTION LIST

No. of Copies	Organization	No. of Copies	Organization
1	Miss Margaret W. Imbrie E. I. DuPont de Nemours and Company Eastern Laboratory Library Drawer G Gibbstown, New Jersey	1	Professor E. M. Pugh Carnegie Institute of Technology Department of Physics Pittsburgh, Pennsylvania
1	Dr. G. Sargent Janes AVCO Manufacturing Corporation Advanced Development Division, Research Laboratory 2385 Revere Beach Parkway Everett 49, Massachusetts	1	Dr. R. J. Reithel University of California Los Alamos Scientific Laboratory Los Alamos, New Mexico
1	Professor Jack Katzenstein The University of New Mexico Albuquerque, New Mexico	1	Mr. Zoltan Rieder Yeshiva University Graduate School of Mathematical Sciences Amsterdam Avenue & 186th Street New York 33, New York
1	Dr. R. C. Maninger Librascope, Incorporated Livermore, California	1	Dr. Carl A. Rouse University of California Lawrence Radiation Laboratory Theoretical Division P. O. Box 808 Livermore, California
1	Professor R. A. Marcus Polytechnic Institute of Brooklyn Brooklyn, New York	1	Dr. Daniel Schiff Raytheon Manufacturing Company Advanced Development Laboratory
1	Dr. Earle B. Mayfield U. S. Naval Ordnance Test Station Michelson Laboratory China Lake, California		Government Equipment Division Waltham, Massachusetts
1	Dr. Frank W. Neilson Sandia Corporation Sandia Base P. O. Box 5800 Albuquerque, New Mexico	1	Dr. G. T. Skinner Cornell Aeronautical Laboratory, Inc. 4455 Genessee Street Buffalo 5, New York
		1	Mr. W. L. Starr Lockheed Aircraft Corporation Missiles and Space Division Palo Alto, California
1	Dr. Luther E. Preuss Edsel B. Ford Institute for Medical Research Department of Physics Detroit 2, Michigan	1	Dr. Alvin Tollestrup California Institute of Technology Pasadena, California
1	Dr. A. E. Puckett Hughes Aircraft Company Culver City, California		

DISTRIBUTION LIST

No. of Copies	Organization	No. of Copies	Organization
1	Dr. T. J. Tucker Sandia Corporation Sandia Base P. O. Box 5800 Albuquerque, New Mexico	1	Dr. Martin Keilhacker Laboratorium fur Technische Physik der Technischen Hochschule Menchen München 2, Germany
1	Mr. E. E. Walbrecht Picatinny Arsenal Explosive Research Section Dover, New Jersey	1	Dr. Werner Muller Ministry for Defense Meppen (ems), Germany
1	Dr. Francis H. Webb California Institute of Technology Pasadena, California	1	Dr. Herbert Oertel French-German Laboratorie de Recherches Techniques de Saint-Louis, France
1	Dr. Victor Wouk, President Electronic Energy Conversion Corp. Box 86 New York 29, New York	1	Dr. K. Oshima Aeronautical Research Institute University of Tokyo Tokyo, Japan
1	Dr. L. Zernow Aerojet-General Corporation Azusa, California	1	Dr. H. Reichenbach Ernst Mach Institut Freiburg im Bresisgan, Germany
1	Monopole des Poudres ATTN: Mr. G. Auniz 12, Quai Henri-IV Paris (IVE), France	1	Dr. A. Sakurai Tokyo Electrical Engineering College Kanda, Tokyo, Japan
1	Professor Dr. H. Bartels Physikalisches Institut Hannover, Germany Welfengarten 1	1	Dr. A. Watson Research Department Arc Physics Section Associated Electrical Industries, Ltd. Trafford Park Manchester 17, England
1	Dr. Erwin David French-German Laboratorie de Recherches Techniques de Saint-Louis, France		

AD _____ Accession No. _____

Ballistic Research Laboratories, APG
TRANSIENT SKIN EFFECTS IN EXPLODING WIRE CIRCUITS
F. D. Bennett

BRL Report No. 1137   August 1961

DA Proj No. 503-03-009, OMSC No. 5210.11.140
UNCLASSIFIED REPORT

Aerodynamics Testing
Equipment
Exploding Wires -
Measurements

The transient response of the coaxial, current-measuring shunt commonly used in high-current, high frequency applications (up to 1 mc) is analyzed by Laplace transform methods. An approximate solution is obtained which allows estimates to be made of the errors expected. The current shunt measuring a damped oscillation will always report an initial current slope of zero, and the maximum rate of current rise is sensed shortly after switch-on. It is several percent low in typical cases. At the first current maximum, the shunt reading is a few tenths percent high and lags the impressed current by a small fraction of a cycle. The transient resistance of an idealized plate condenser is analyzed using the asymptotic solution for current. A numerical calculation indicates no alteration of initial conditions on the damped oscillation to arise from this source, so long as the characteristic damping time of the transient skin effect is small compared with the ringing time.

AD   Accession No.   UNCLASSIFIED
Ballistic Research Laboratories, APG
TRANSIENT SKIN EFFECTS IN EXPLODING WIRE CIRCUITS   Aerodynamics Testing
F. D. Bennett   Equipment
                                                        Exploding Wires -
BRL Report No. 1137 August 1961   Measurements

DA Proj No. 503-03-009, OMSC No. 5210.11.140
UNCLASSIFIED REPORT

The transient response of the coaxial, current-measuring shunt commonly
used in high-current, high frequency applications (up to 1 mc) is analyzed
by Laplace transform methods. An approximate solution is obtained which
allows estimates to be made of the errors expected. The current shunt
measuring a damped oscillation will always report an initial current slope of
zero, and the maximum rate of current rise is sensed shortly after switch-on.
It is several percent low in typical cases. At the first current maximum, the
shunt reading is a few tenths percent high and lags the impressed current by a
small fraction of a cycle. The transient resistance of an idealized plate
condenser is analyzed using the asymptotic solution for current. A numerical
calculation indicates no alteration of initial conditions on the damped
oscillation to arise from this source, so long as the characteristic damping
time of the transient skin effect is small compared with the ringing time.

AD   Accession No.   UNCLASSIFIED
Ballistic Research Laboratories, APG
TRANSIENT SKIN EFFECTS IN EXPLODING WIRE CIRCUITS   Aerodynamics Testing
F. D. Bennett   Equipment
                                                        Exploding Wires -
BRL Report No. 1137 August 1961   Measurements

DA Proj No. 503-03-009, OMSC No. 5210.11.140
UNCLASSIFIED REPORT